MicroRNA-421 promotes the progression of non-small cell lung cancer by targeting HOPX and regulating the Wnt/β-catenin signaling pathway

HUAGANG LIANG*, CHAO WANG*, KUN GAO, JIAN LI and RUI JIA

Department of Thoracic Surgery, The First Hospital of Qinhuangdao, Qinhuangdao, Hebei 066000, P.R. China

Abstract. MicroRNAs (miRNAs) function as key regulators of numerous types of cancers. miRNA (miR)-421 expression is dysregulated in a variety of tumors; however, its role in non-small cell lung cancer (NSCLC) remains unclear. In the present study, the role and molecular mechanism of miR-421 in NSCLC was investigated. In this study, miRNA (miR)-421 was upregulated in NSCLC tissues and cell lines used the reverse transcriptase quantitative polymerase chain reaction. Ectopic expression of miR-421 significantly promoted cell proliferation *in vitro* and tumor growth *in vivo* by promoting cell cycle progression via CCK-8, colony formation, EdU assay, xenograft model and cell cycle assay. In addition, miR-421 inhibited NSCLC cell apoptosis by flow cytometry apoptosis assay, as evidenced by anti-apoptosis gene Bcl-2 and apoptosis gene cleaved caspase-3 and cleaved PARP using western blot assay. Furthermore, miR-421 promoted cell migration and invasion through EMT process using Transwell and western blot assay. It was also demonstrated that miR-421 can directly target HOPX by the EGFP reporter assay and western blot assay. MiR-421 overexpression promoted the protein expression levels of β-catenin, cyclin D1 and c-myc by western blot assay, which are the downstream genes of Wnt pathway. These data indicated that miR-421 may act as an oncogene through the effects of HOPX on the Wnt/β-catenin signaling pathway and may provide insight into the mechanisms underlying carcinogenesis and the identification of potential biomarkers associated with NSCLC.

Correspondence to: Dr Huagang Liang, Department of Thoracic Surgery, The First Hospital of Qinhuangdao, 258 Wenhua Road, Qinhuangdao, Hebei 066000, P.R. China
E-mail: lianghgarticles@163.com

*Contributed equally

Introduction

Lung cancer is one of the most prevalent types of malignant tumors, and has been reported to be the leading cause of cancer-associated mortality worldwide, particularly in China (1,2). Lung cancer is divided into two classes, according to the degree of differentiation and morphologic characteristics: i) Small cell lung cancer and ii) non-small cell lung cancer (NSCLC). As the most common subtype of lung cancer, NSCLC accounts for 85% of lung cancer cases (3). The high rates of mortality for NSCLC have been associated with smoking; a large number of patients with NSCLC succumb to metastasis (4). Advances in treatments for NSCLC have been achieved, including surgery, radiotherapy and chemotherapy; however, the 5-year survival rate of patients with NSCLC is <15% and prognosis remains poor (5,6). Therefore, it is important to investigate and identify novel biomarkers, and to develop novel therapeutic strategies for the treatment of NSCLC.

MicroRNAs (miRNAs) are a group of short, regulatory non-coding RNA molecules of ~22 nucleotides in length (7). The action of miRNAs results in translational suppression or mRNA degradation by targeting complementary sequences of the mRNA 3'-untranslated region (UTR) (7). In addition, miRNAs serve key roles in a number of processes, including cell proliferation, apoptosis, motility and metastasis (7-9). Each miRNA regulates the expression of potentially hundreds of different genes, and have been reported to exhibit opposing roles in numerous types of cancer (10,11). miRNAs may serve as novel therapeutic agents for the treatment of cancers, as they can function as tumor suppressors or as oncogenes (12). In particular, miRNA (miR)-421 has also been reported to exhibit dual roles in various types of cancer. For example, downregulation of miR-421 may act as a tumor suppressor; miR-421 was demonstrated to inhibit glucose metabolism, invasion and angiogenesis, as well as enhance the radiation sensitivity by targeting myocyte enhancer factor 2D in glioma (13). Conversely, miR-421 has been observed to be frequently upregulated and function as an oncogene; miR-421 was reported to promote metastasis, inhibit apoptosis and induce cisplatin resistance by targeting E-cadherin and caspase-3 expression in gastric cancer (14). Therefore, the present study aimed to investigate whether miR-421 may affect the malignant phenotypes of NSCLC.

In the present study, miR-421 was upregulated in NSCLC tissue samples and cells. MiR-421 functions as an oncogene in NSCLC cells. Furthermore, miR-421 could directly target HOPX in NSCLC cells. The present study confirmed that the homeodomain-only protein (HOPX) gene may be a direct functional target of miR-421. miR-421 was observed to suppress HOPX expression, which may contribute to the development of malignant properties through the Wnt/β-catenin signaling pathway in NSCLC cells. These results may provide insight into the mechanisms underlying carcinogenesis and the identification of potential biomarkers associated with NSCLC.

Materials and methods

Human NSCLC tissue specimens and cell lines. Tumor and normal paired tissue samples were collected from 30 patients with NSCLC from December 2016 to June 2017 at the Department of Thoracic Surgery, The First Hospital of Qinhuangdao, including 10 females and 20 males whose age from 35 to 67 years old. Patients did not receive therapy at the time of sample collection. Written informed consent was obtained from all enrolled patients, and all relevant investigations were performed according to the principles of The Declaration of Helsinki. The present study was approved by the Ethical Review Committee of The First Hospital of Qinhuangdao (ethics approval no. QHD20160235). The human NSCLC cell lines A549, H358, H460, H2066, SPC-A1 and a normal human primary lung fibroblast cell line, HLF-a (ATCC® CCL-199™) were purchased from the Cell Bank of Type Culture Collection of Chinese Academy of Sciences (Shanghai, China) and cultured in MEM-a (HyClone; GE Healthcare, Chicago, IL, USA) medium supplemented with 10% fetal bovine serum (FBS; Gibco; Thermo Fisher Scientific, Inc., Waltham, MA, USA). All cells were incubated in a humidified atmosphere with 5% CO_2 at 37˚C.

Prediction of miRNA targets. Algorithm programs, including Human TargetScan7.2, microrna.org and miRDB were used to predict the target genes of miR-421.

Vector construction. The DNA fragment encoding primary (pri)-miR-421 was cloned into the mammalian expression vector pcDNA3 (Promega Corporation, Madison, WI, USA) at *Bam*HI and *Eco*RI. A 2'-O-methyl-modified antisense oligonucleotide of miR-421 (ASO-miR-421) was commercially synthesized to serve as an inhibitor of miR-421 (Genewiz, South Plainfield, NJ, USA). The cDNA fragment containing the HOPX coding sequence (cat. no. BC014225; Tianjin Saier Corporation, Tianjin, China) was amplified by polymerase chain reaction (PCR). The subsequent PCR product was cloned into the pcDNA3 vector at *Bam*HI and *Eco*RI, thus generating the HOPX expression plasmid (pHOPX). In addition, enhanced green fluorescent protein (EGFP) reporter plasmids (pcDNA3/EGFP, Tianjin Saier Corporation, Tianjin, China) with the wild-type HOPX 3'UTR (HOPX-WT) containing the target site of miR-421 or the mutant (HOPX-Mut) were constructed, respectively. The 3'UTR of HOPX that contain the miR-421 binding sites and mutant 3'UTR fragments with mutant miR-421 binding sites (site-directed mutagenesis) were obtained by annealing double-strand DNA and inserting it into the pcDNA3/EGFP vector. All primer sequences are listed in Table I.

Cell transfection. A549 cells or SPC-A1 cells ($4x10^5$) were plated in 6-well plates overnight to ensure that cell confluence could reach 60-80% at the time of transfection. Following 6 h transfection at 37˚C, the medium was replaced with MEM-a media containing 10% FBS. Lipofectamine 2000 (Invitrogen; Thermo Fisher Scientific Inc.) was employed in cell transfection according to the manufacturer's protocol. They were transiently transfected with 3ug pri-miR-421 or pcDNA3 and 20 μmol ASO-miR-421 or ASO-NC in a well of 6-well plate. Cells were collected for reverse transcription-quantitative PCR (RT-qPCR), proliferation, migration, invasion, apoptosis and cell cycle assay analyses at 24 h. At 48 h post-transfection, cells were collected for western blot analysis and the EGFP fluorescent reporter assay.

RNA extraction and RT-qPCR. Total RNA was extracted for $8x10^5$ cells using the TRIzol® reagent (Invitrogen; Thermo Fisher Scientific, Inc.), according to the manufacturer's protocol. cDNA was prepared using the PrimeScript RT Reagent kit (Takara Biotechnology Co., Ltd., Dalian, China) according to the manufacturer's protocol. Subsequently, cDNA was used to detect mRNA expression levels by qPCR using the SYBR® Premix Ex Taq™ II Perfect Real-Time kit (Takara Biotechnology Co., Ltd.) and an ABI 7500 Real-time PCR system (Applied Biosystems; Thermo Fisher Scientific, Inc.). The thermos cycling conditions for RT-qPCR were as follows: 95˚C for 20 sec, followed by 35 cycles of 95˚C for 5 sec, 63˚C for 30 sec and 72˚C for 5 sec. Gene expression levels of HOPX and miR-421 were normalized to that of endogenous β-actin (for HOPX) or U6 (for miR-421), respectively. The relative fold changes in the transcript levels were calculated using the $2^{-\Delta\Delta Cq}$ method [15]. The primers used for RT-qPCR are presented in Table I.

EGFP fluorescent reporter assay. A total of $2x10^4$ A549 and SPC-A1 cells were seeded in 48-well plates and co-transfected with $0.5\,\mu g$ pri-miR-421, $0.5\,\mu g$ pcDNA3, 20 nM ASO-miR-421 or 20 nM ASO-NC with 0.5 μg EGFP-HOXP-WT or 0.5 μg EGFP-HOXP-Mut 3'UTR plasmids, as aforementioned. A pDsRed2-1 vector (0.1 g/well) encoding red fluorescent protein (RFP; Clontech Laboratories, Inc., Mountain View, CA, USA) was used for normalization. At 48 h post-transfection, the fluorescence intensities of EGFP and RFP were detected at 528 and 488 nm using an F-4500 Fluorescence Spectrophotometer (Hitachi, Ltd., Tokyo, Japan).

Western blotting. Western blotting was conducted in the present study as previously described [16]. Briefly, A549 cells ($6x10^8$) were washed with 1X PBS buffer and lysates were prepared with Radio-immunoprecipitation Assay Buffer (Beyotime Institute of Biotechnology, Shanghai, China), and protein concentrations were quantified using a Bicinchoninic Acid Protein Assay kit (Beyotime Institute of Biotechnology), according to the manufacturer's protocols. Protein samples (25 μg) were separated by 12% SDS-PAGE and subsequently transferred to polyvinylidene difluoride membranes. Subsequently, the membranes were blocked with 5% non-fat milk in 1X Tris-buffered saline with 0.05% Tween-20 for ~2 h at room temperature, followed by incubation at 4˚C overnight with the following primary

Table I. Primers used in the present study.

A, Plasmid primers

Primers	Primer sequence (5'→3')
pri-miR-421	F: CGCGGATCCAGCAGCAACCTGGAGTGG
	R: CCGGAATTCGAGCTTGGACGTTGTTGG
HOPX-3'UTR-WT	F: GATCCCGCGGGTTAATTACAGACAACTAAAGCTTG
	R: AATTCAAGCTTTAGTTGTCTGTAATTAACCCGCGG
HOPX-3'UTR-Mut	F: GATCCCGCGGAAGAATTACTGTTAGGGAAAGCTTG
	R: AATTCAAGCTTTCCCTAACAGTAATTCTTCCGCGG
HOPX	F: CGCGGATCCATGCTCATTTTCCTGGGCTGTTACA
	R: CCGGAATTCTTAGTCTGTGACGGATCTGCACTCT

B, RT-qPCR primers

Primers	Primer sequence (5'→3')
miR-421-RT	GTCGTATCCAGTGCAGGGTCCGAGGTGCACTGGATACGAGCGCCC
miR-421-qPCR-F	TGCGGATCAACAGACATTAAT
U6-RT	GTCGTATCCAGTGCAGGGTCCGAGGTATTC
	GCACTGGATACGACAAAATATGGAAC
Oligo-dT	TTTTTTTTTTTTTTTTTT
U6-F	TGCGGGTGCTCGCTTCGGCAGC
miRNA-universal-R	CCAGTGCAGGGTCCGAGGT
HOPX	F: AGCATTTCCCTTTGAGTC
	R: GCCCAACAGGCTTCTTTC
β-actin	F: CGTGACATTAAGGAGAAGCTG
	R: CTAGAAGCATTTGCGGTGGAC

F, forward; HOPX, homeodomain-only protein; miR, microRNA; Mut, mutant; pri, primary; qPCR, quantitative polymerase chain reaction; R, reverse; RT, reverse transcription; UTR, untranslated region; WT, wild-type.

antibodies (unless otherwise noted, all antibodies were from Wanlei Bio Co., Ltd., Beijing, China; www.wanleibio.cn/): Anti-GAPDH (1:2,000; cat. no. WL01547); anti-E-cadherin (1:1,000; cat. no. WL01482); anti-vimentin (1:1,000; cat. no. WL00742); anti-Bcl-2 (1:1,000; cat. no. WL01556); anti-cleaved caspase-3 (1:1,500; cat. no. WL01556); anti-cleaved PARP (1:1,000; cat. no. WL01932); anti-β-catenin (1:1,000; cat. no. WL01160); anti-phosphorylated β-catenin (1:1,000; cat. no. ab27798; Abcam, Cambridge, UK); anti-cyclin D1(1:2,000; cat. no. WL01435a); and anti-c-myc (1:3,000; cat. no. WL01781). Following three extensive washes with PBS+Tween-20 (0.1%) for 20 min at room temperature, the membranes were incubated with polyclonal goat anti-rabbit horseradish peroxidase-conjugated secondary antibody (1:5,000; cat. no. ab98512; Abcam) for 2 h at room temperature, followed by three washes with PBS+Tween-20 for 20 min at room temperature. Protein bands were visualized using an Enhanced Chemiluminescence Detection kit (Sigma-Aldrich; Merck KGaA, Darmstadt, Germany), and images were captured using LabWorks™ Image Acquisition (UVP, Inc., Upland, CA, USA). Analysis Software UVP EC3 v3.0 software (UVP, LLC,

Phoenix, AZ, USA) were used to quantify band intensities and GAPDH was used to normalize protein expression levels.

Cell Counting Kit-8 (CCK-8) and colony formation assays. Cell proliferation was determined by a CCK-8 assay (cat. no. WLa074a; Wanlei Bio, Co., Ltd.). At 24 h post-transfection, A549 or SPC-A1 cells (5,000 cells/well) were seeded in 96-well plates and cultured for 24, 48 or 72 h. A total of 10 μl CCK-8 reagent was added to each well, and the plates were incubated at 37°C for an additional 6 h. The optical density (OD) at a wavelength of 450 nm was determined using a microplate reader (Hitachi, Ltd.). The OD values reflect the relative number of viable cells. For the colony formation assay, A549 or SPC-A1 cells (2×10^3 cells/well) were seeded onto 12-well plates and incubated for 10-14 days. The colonies were then fixed in 100% methanol for 30 min, stained with crystal violet for 30 min at room temperature and the numbers of macroscopically observable colonies were recorded.

Transwell migration and invasion assays. Briefly, A549 and SPC-A1 cells were seeded into 8-μm cell culture inserts and

placed in 24-well Transwell cell culture plates. The upper chamber was coated with 100 μl diluted Matrigel (2 mg/ml) for invasion assay. The lower chamber was filled with 500 μl of MEM-a medium containing 20% FBS. A549 and SPC-A1 cells (6×10^4) in 200 μl of serum-free MEM-a medium were gently each filter insert (loaded onto upper chamber) and incubated at 37˚C for 48 h. The filter inserts were removed from the chambers and the non-migrative cells were removed using the cotton swab, fixed with methanol for 10 min and stained with Harris' hematoxylin for 20 min. The samples were subsequently washed using the 0.9% saline solution, dried and mounted onto slides. The migratory and invasive cells were stained blue and six random fields were examined under an inverted microscope (magnification, x200) for statistical analysis.

Cell cycle and apoptosis analysis by flow cytometry. A549 and SPC-A1 cells were washed with cold 1X PBS. After washing with PBS, 1×10^6 cells were fixed in 100% ethanol for 10 min and incubated with 50 μg/ml propidium iodide (PI; Nanjing KeyGen Biotech; www.keygentec.com.cn) for 10 min at room temperature in the dark and analyzed within 20 min using a BD FACSCalibur (BD Biosciences, Franklin Lakes, NJ, USA). Flow cytometry was used to detect cell apoptosis and analyzed using FlowJo 7.6.1 (FlowJo LLC, Ashland, OR, USA). For cell apoptosis, cells were collected for determination of apoptosis rates using the Annexin V-FLUOS Kit (Nanjing KeyGen Biotech Co., Ltd., Nanjing, China), according to the manufacturer's protocols. All samples were assayed in triplicate.

5-Ethynyl-2'-deoxyuridine (EdU) staining. EdU staining was performed using the Click-iT EdU Imaging kit (Invitrogen; Thermo Fisher Scientific, Inc.), according to the manufacturer's protocols. In brief, A549 and SPC-A1 were plated in 96-well plates. After the required treatment, EdU was added into each well and incubated for 3 h. After washing twice with PBS, the cells were fixed with 4% paraformaldehyde for 30 min at room temperature. Then, cells were incubated with Apollo staining reaction liquid for 30 min to detect the positive cells. The cells were counterstained with 50 nM Hoechst 33342 at room temperature. Immunofluorescence was observed with a fluorescence microscope (DMI 3000B; Leica Microsystems GmbH, Wetzlar, Germany).

Immunofluorescent microscopy. Transfected cells were seeded (2×10^3 cells/well) into 14-well chambers and incubated for 24 h; the cells were washed with 1X PBS, fixed with 4% paraformaldehyde, permeabilized with 0.5% Triton X-100 and incubated with 10% donkey serum (Beijing Solarbio Science & Technology Co., Ltd., Beijing, China) for 1 h. Subsequently, cells were incubated with rabbit anti-β-catenin antibody (1:100; cat. no. WL01160; Wanlei Bio Co., Ltd.) at 4˚C overnight. The cells were stained for 1.5 h in the dark at room temperature with a fluorescein isothiocyanate-conjugated secondary antibody (1:300; cat. no. ab150077; Goat Anti-Rabbit IgG H&L Alexa Fluor® 488; Abcam). Nuclei were counterstained with DAPI (1:1,000; Sigma-Aldrich; Merck KGaA) for 5 min in the dark at room temperature. The slides were observed by fluorescent microscopy (DMI 3000B; Leica Microsystems GmbH) at 488 and 528 nm through the oil microscope (magnification, x1,000).

Xenograft tumor formation assay. Animal protocols were approved by The First Hospital of Qinhuangdao Animal Care and Use Committee (Qinhuangdao, China); all animals received human care according to the Institutional Animal Care and Treatment Committee of First Hospital of Qinhuangdao (2016N185), and experiments were conducted in accordance with the approved guidelines. Female BALB/c athymic nude mice [four mice/group, two group (n=8); age, 6 weeks; weight, >20 g] were purchased from The Institute of Zoology, Chinese Academy of Sciences (Shanghai, China) were and maintained at 18-29˚C, with relative humidity of 50-60%, 10-14-h light/dark cycle (lights turned on at 8:00 every day and turned off at 18:00), and free access to clean food and water. A total of 2×10^6 stably transfected (pcDNA3 or pri-miR-421) A549 cells were implanted subcutaneously into the armpit of each mouse. All mice were euthanized with CO_2 at 30 days post-implantation. Tumor weights were measured using an electronic scale.

TOP/FOP flash reporter assays. To determine the transcriptional activity of the Wnt pathway, 5×10^6 A549 and SPC-A1 cells treated as indicated were co-transfected with either the Wnt signaling reporter TOP Flash or the negative control FOP Flash (EMD Millipore, Billerica, MA, USA) according to the manufacturer's protocol. A549 and SPC-A1 cells were transiently transfected with either 2 μg pTOP flash or pFOP flash plasmids and 0.5 μg pSV40-*Renilla* plasmid as an internal control (Promega Corporation) using Lipofectamine® 2000 (Invitrogen; Thermo Fisher Scientific, Inc.) at room temperature for 48 h. The dual-luciferase reporter assay system (Dual-Luciferase® Reporter Assay system; cat. no. E1910; Promega Corporation) was used to assay the firefly and *Renilla* luciferase activity ratio.

Statistical analyses. Each experiment was performed in triplicate. The differences between two groups were analyzed using a two-tailed Student's t-tests; multiple group comparisons were performed via two-way analysis of variance followed by the Bonferroni post hoc test. All analyses were performed using SPSS 19.0 for Windows (IBM Corp., Armonk, NY, USA) and GraphPad Prism 5 for Windows (GraphPad Software Inc., La Jolla, CA, USA). P<0.05 was considered to indicate a statistically significant difference.

Results

miR-421 is upregulated in NSCLC tissues and cell lines. RT-qPCR analysis was performed to examine the expression levels of miR-421 in NSCLC tissue and cell lines. The results demonstrated that the expression levels of miR-421 were significantly increased in 30 pairs of NSCLC tissues compared with expression levels in the adjacent non-cancerous tissues (Fig. 1A). Similarly, compared with in a normal human primary lung fibroblast cell line, HLF-a, all NSCLC cell lines (A549, H358, H460, H2066 and SPC-A1) exhibited significantly higher expression levels of miR-421 (Fig. 1B). A549 and SPC-A1 cell lines were selected for further study, because they were easier to culture and transfect compared with in the other NSCLC cell lines.
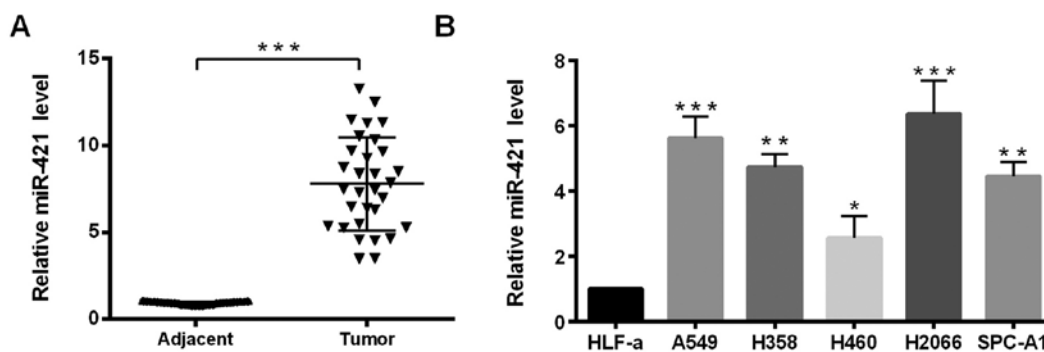
Figure 1. Differential expression of miR-421 in NSCLC tissues and cells. (A) Relative expression levels of miR-421 in 30 paired NSCLC and adjacent non-cancerous tissues were determined by RT-qPCR; U6 was used for normalization; ***P<0.001. (B) Expression levels ofmiR-421 in different NSCLC cell lines and the normal human primary lung fibroblast cell line HLF; U6 was used for normalization. Data are presented as the mean ± standard deviation; *P<0.05, **P<0.01 and ***P<0.001 vs. HLF-a. miR, microRNA; RT-qPCR, reverse transcription-quantitative polymerase chain reaction.

miR-421 promotes NSCLC cell growth, migration and invasion in vitro. As miR-421 expression levels in NSCLC tissues and cell lines were high, it was hypothesized that miR-421 may function as an oncogene in the progression of NSCLC. First, the miR-421 overexpression plasmid and the synthesized ASO-miR-421 were used, and the efficiency of the plasmids was confirmed in A549 and SPC-A1 cells by RT-qPCR (Fig. 2A); that is, miR-421 expression levels were increased and decreased, respectively, compared with the negative controls. Subsequently, the effects of miR-421 on the malignant behaviors of NSCLC cells were also investigated. Results from CCK-8 and colony formation assays demonstrated that miR-421 overexpression significantly promoted cell viability and colony formation (Fig. 2B and C, respectively), whereas viability and colony formation were significantly inhibited in cells transfected with ASO-miR-421 compared with the respective pcDNA3 empty vector and ASO-NC groups in the two cells lines. To investigate how miR-421 may promote A549 and SPC-A1 cell growth, the effects of miR-421 on the cell cycle were analyzed. The cell cycle distribution of A549 and SPC-A1 cells was observed to be affected by alterations in miR-421 expression (Fig. 2D). EdU was used to examine cell proliferation, the result showed that pri-miR-421 promoted the EdU concentration and ASO-miR-421 reduced the EdU concentration compared with the control groups in A549 and SPC-A1 cells (Fig. 2E). To investigate whether miR-421 affected the motility of NSCLC cells, Transwell migration and invasion assays were performed using transfected A549 and SPC-A1 cells. The migratory and invasive abilities of A549 and SPC-A1 cells transfected with pri-miR-421 were notably increased, and cells transfected with ASO-miR-421 were notably decreased compared with the corresponding control-transfected cells (Fig. 2F).

Previous studies suggested that EMT serves important role in cancer metastasis (17). During the EMT process, a loss of epithelial markers and the acquisition of mesenchymal markers have been observed (18). Therefore, the present study evaluated the role of miR-421 in the EMT process. Western blot analysis revealed that the expression levels of E-cadherin were significantly decreased and that of vimentin was significantly increased in miR-421-overexpressing cells compared with the pcDNA3 transfected group; ASO-miR-421 transfection induced a significant increase in E-cadherin and a

significant decrease in vimentin expression levels within A549 cells compared with the ASO-NC transfected group (Fig. 2G). Collectively, these data indicated that miR-421 may promote the EMT process, as well as the migration and invasion of NSCLC cells. In addition, the rate of cell apoptosis was examined. The apoptotic rates of A549 and SPC-A1 cells were significantly decreased in response to miR-421 overexpression, whereas the downregulation of miR-421 expression levels by ASO-miR-421 led to increased rates of cell apoptosis (Fig. 2H). Additionally, western blotting results indicated that miR-421 overexpression significantly upregulated the expression levels of Bcl-2, but reduced that of cleaved caspase-3 and cleaved PARP in A549compared with the pcDNA3vector group (Fig. 2I).

HOPX is a target of miR-421. To investigate the mechanism underlying the effects of miR-421 on the malignant phenotypes exhibited by NSCLC cells, the potential targets of miR-421 were predicted using the algorithm programs TargetScan, microrna.org and miRDB. Among the 451 predicted target genes, HOPX was selected or further study as the association between HOPX and NSCLC progression remains unknown.

To confirm whether HOPX is a target of miR-421, fluorescent reporter plasmids with the HOPX-WT or HOPX-Mut 3'UTR fragment were constructed (Fig. 3A). The fluorescence intensity of the HOPX-WT 3'UTR was significantly suppressed when co-transfected with pri-miR-421 compared with cells that were co-transfected with pcDNA3 empty vector (Fig. 3B); whereas the opposite effects were observed when cells were co-transfected with ASO-miR-421 compared with ASO-NC (Fig. 3B). However, these effects were abolished when the potential miR-421 binding sites were mutated (Fig. 3B). The results also demonstrated significantly lower expression of HOPX in cells overexpressing miR-421 (pri-miR-421) and higher expression of HOPX in cells knocking down miR-421 (ASO-miR-421) at the mRNA (Fig. 3C) and protein (Fig. 3D) levels in cells compared with the control group cells. To verify the results obtained from the cell lines, the collected tissues and the NCBI Gene Expression Omnibus database were used for further analysis. The results revealed significantly lower HOPX mRNA expression levels in the NSCLC tissues and in the GEO database, compared with the adjacent normal lung tissues (Fig. 3E and F, respectively). Collectively, these results
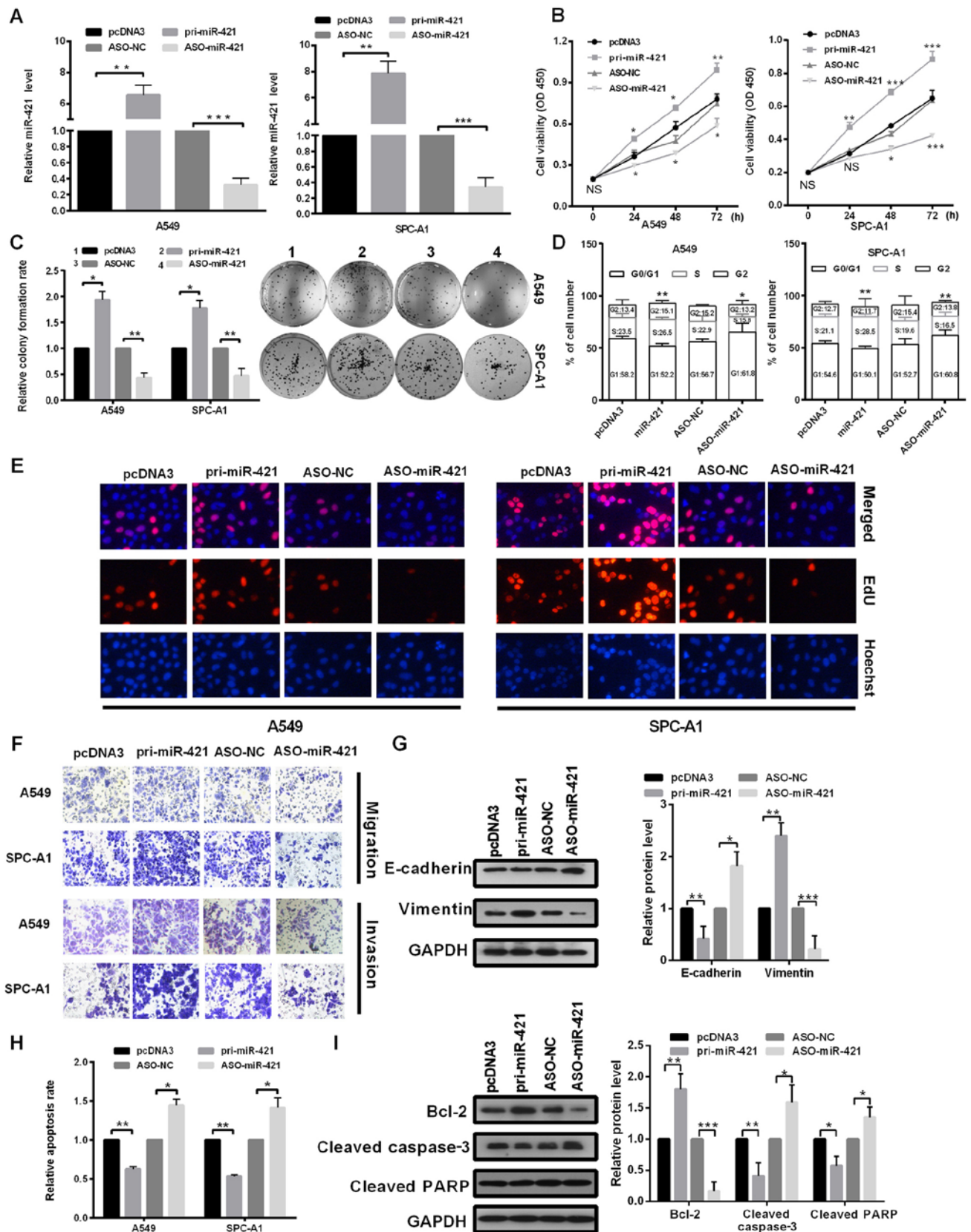
Figure 2. miR-421 contributes to the oncogenic activity of non-small cell lung cancer cells. (A-I) A549 and SPC-A1 cells were transfected with pri-miR-421, pcDNA3, ASO-miR-421 or ASO-NC. (A) Reverse transcription-quantitative polymerase chain reaction was used to detect the mRNA expression levels of miR-421. (B) Viability was examined by Cell Counting Kit-8. (C) Results from colony formation assays. (D) The cell cycle was analyzed by flow cytometry following transfection. (E) EdU cell proliferation assay was performed to assess cell prouliferation; Nuclei were stained with Hoechst 33342. (F) Transwell migration and Matrigel invasion assays. (G) Protein expression levels of E-cadherin and vimentin were detected by western blotting; GAPDH was used as a control and for normalization. (H) Cell apoptosis was analyzed by flow cytometry. (I) Protein expression levels of Bcl-2, cleaved caspase-3 and cleaved PARP were examined by western blotting; GAPDH was used for control normalization. The data are presented as the mean ± standard deviation; *P<0.05, **P<0.01 and ***P<0.001 vs. the respective Control. ASO, antisense oligonucleotide; Bcl-2, B cell lymphoma-2; E-cadherin, epithelial cadherin; EdU, 5-ethynyl-2'-de-oxyuridine; miR, microRNA; NC, negative control; PARP, poly(ADP-ribose) polymerase; pcDNA3, empty vector; pri, primary.
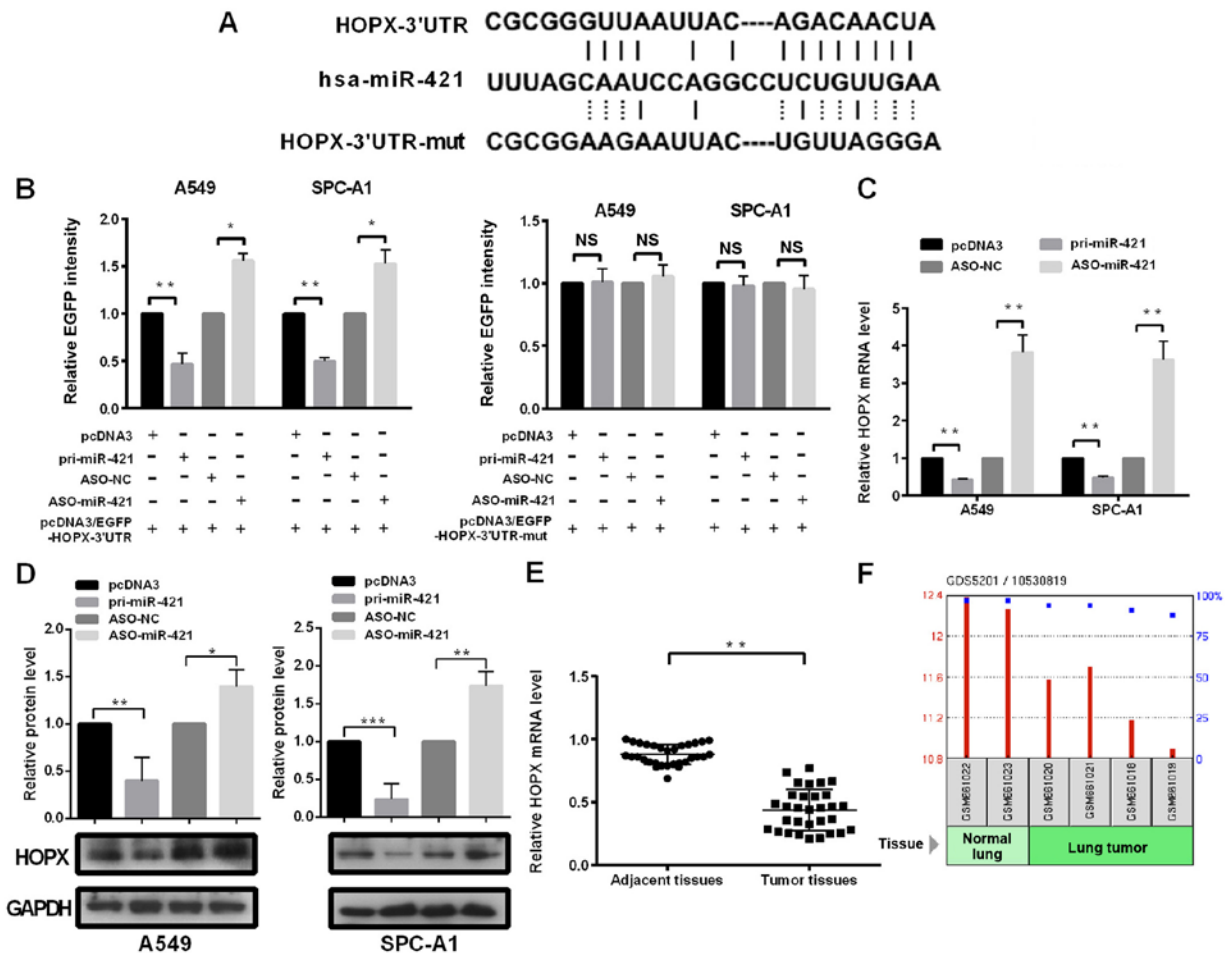
Figure 3. miR-421 targets the HOPX 3'UTR and suppresses its expression. (A) Predicted WT and Mut binding sites for miR-421 in the 3'UTR of HOPX mRNA. (B) A549 and SPC-A1 cells were co-transfected with the HOPX-WT or HOPX-Mut 3'UTR reporter plasmids along with pri-miR-421, pcDNA3, ASO-NC or ASO-miR-421; EGFP fluorescence intensity was measured at 48 h post-transfection and normalized to pDsRed2-N1 vector. (C and D) A549 and SPC-A1 cells were transfected with pri-miR-421, pcDNA3, ASO-miR-421 or ASO-NC and the (C) mRNA and (D) protein expression levels of HOPX were determined by reverse transcription-quantitative polymerase chain reaction and western blotting, respectively. (E and F) Relative expression levels of HOPX in (E) paired non-small cell lung cancer and adjacent non-cancerous tissues, and (F) NCBI Gene Expression Omnibus database. Normal lung tissues and lung cancer tissues. Data are presented as the mean ± standard deviation; *P<0.05, **P<0.01, ***P<0.001. ASO, antisense oligonucleotide; EGFP, enhanced green fluorescent protein; HOPX, homeodomain-only protein; miR, microRNA; Mut, mutant; NC, negative control; NS, not significant; pcDNA3, empty vector; pri, primary; UTR, untranslated region; WT, wild-type.

indicated that HOPX may be negatively regulated by miR-421 in NSCLC cells.

HOPX rescues the effects of miR-421 on the malignant behaviors of NSCLC cells. As HOPX was predicted to be a direct target of miR-421 in NSCLC, whether miR-421 may function as an oncogene in a HOPX-dependent manner was investigated. Prior to performing the functional studies, a HOPX overexpression vector, pHOPX, was generated and the efficiency of transfection of A549 and SPC-A1 cells was analyzed by RT-qPCR (Fig. 4A); the results confirmed that HOPX mRNA expression levels were increased compared with the Control-transfected cells. Subsequently, the effects of HOPX on NSCLC cell viability, growth, migration and invasion were investigated. Ectopic expression of HOPX inhibited cell viability, growth, proliferation, migration, invasion and EMT, induced cell apoptosis compared with the pcDNA3+pcDNA3 group (Fig. 4B-I). These results suggested that HOPX may suppress various malignant phenotypes of NSCLC cells *in vitro*, and serve an opposing role to miR-421.

To confirm that the phenotype of miR-421 may arise from the suppression of HOPX expression, rescue experiments were performed. HOPX partially suppressed the viability, growth, proliferation migration, invasion of NSCLC cells, counteracting the promoting effects on the malignant phenotype induced by miR-421 (Fig. 4B-I). Collectively, these data demonstrated that HOPX may be an important functional target gene in NSCLC cells.

miR-421 regulates the Wnt/β-catenin signaling pathway mediated by HOPX. Chromatin immunoprecipitation-sequencing analyses have revealed that HOPX binds to Wnt target genes, which indicated that HOPX may be involved in the Wnt/β-catenin signaling pathway (19). The overexpression of miR-421 significantly induced, whereas ectopic expression of HOPX significantly decreased phosphorylated β-catenin expression compared with pcDNA3 vector-transfected cells (Fig. 5A); no significant differences were observed for total β-catenin expression. This result suggested that miR-421 may induce the Wnt/β-catenin signaling pathway.
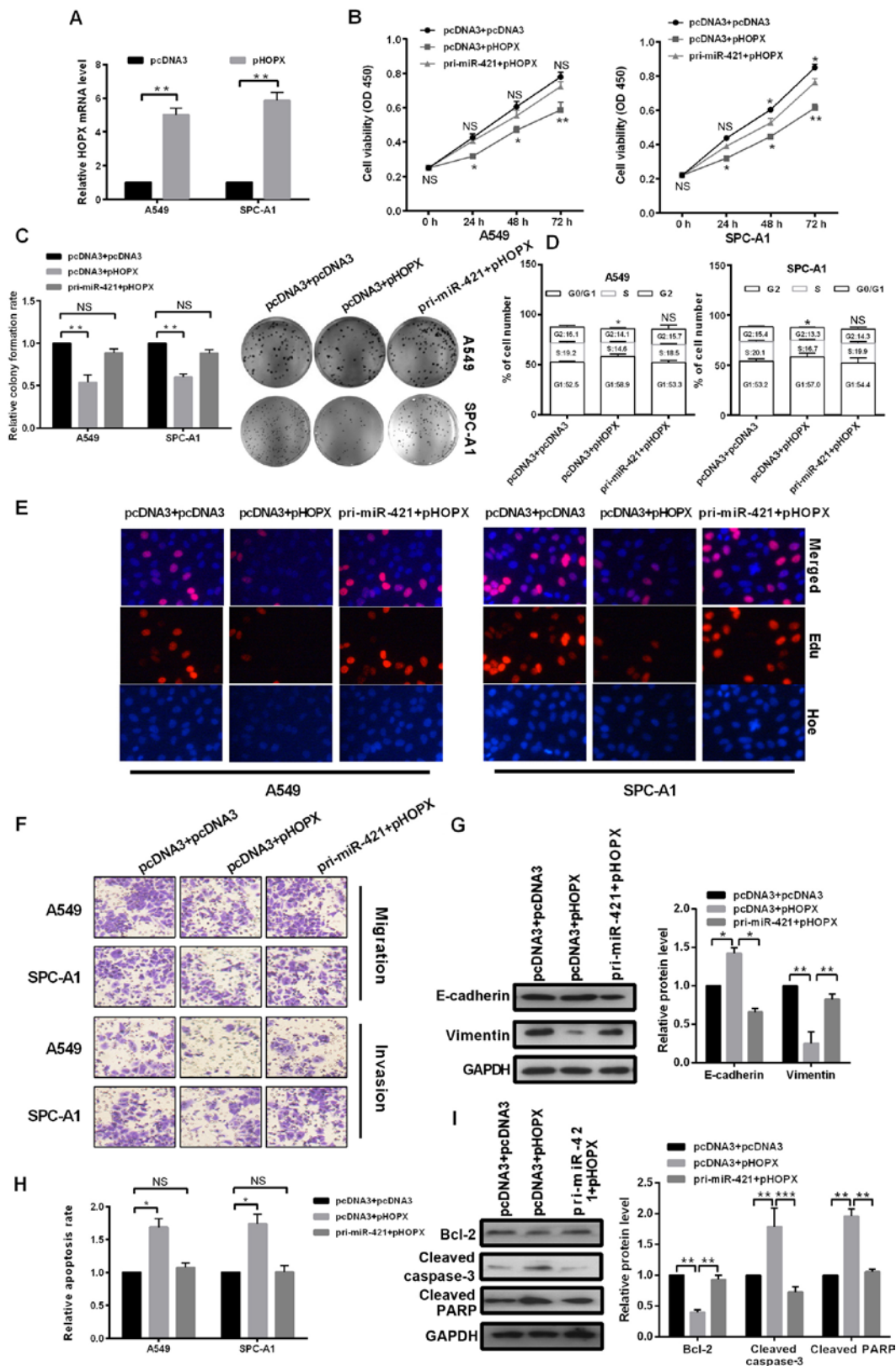
Figure 4. HOPX overexpression reverts miR-421-mediated cell growth and metastasis-associated traits. (A) Expression levels of HOPX were analyzed by reverse transcription-quantitative polymerase chain reaction to confirm successful transfection of the pHOPX overexpression vector in A549 and SPC-A1 cells; β-actin was used for normalization. (B-I) A549 and SPC-A1 cells were co-transfected with pcDNA3+pHOPX or pri-miR-421+pHOPX compared with the pcDNA3+pcDNA3 group. (B) Cell viability was determined by Cell Counting Kit-8. (C) Colony formation assay. (D) Cell cycle analysis was detected by flow cytometry. (E) EdU assay was performed to assess the proliferative ability of transfected cells; nuclei were stained with Hoechst 33342. (F) Effects on cell migration and invasion were examined by Transwell and Matrigel assays, respectively. (G) Protein expression levels of epithelial-mesenchymal transition-associated markers E-cadherin and vimentin were examined by western blotting; GAPDH was used as a loading control and for normalization. (H) Rate of apoptosis was determined via flow cytometry. (I) Protein expression levels of Bcl-2, cleaved caspase-3 and cleaved PARP were analyzed by western blotting. Data are presented as the mean ± standard deviation; $^{*}P<0.05$, $^{**}P<0.01$ and $^{***}P<0.001$. ASO-NC, antisense negative control; ASO, antisense oligonucleotide; Bcl-2, B cell lymphoma-2; E-cadherin, epithelial cadherin; EdU, 5-ethynyl-2'-deoxyuridine; HOPX, homeodomain-only protein; miR, microRNA; NS, not significant; PARP, poly(ADP-ribose) polymerase; pcDNA3, empty vector; pHOPX, HOPX overexpression vector.
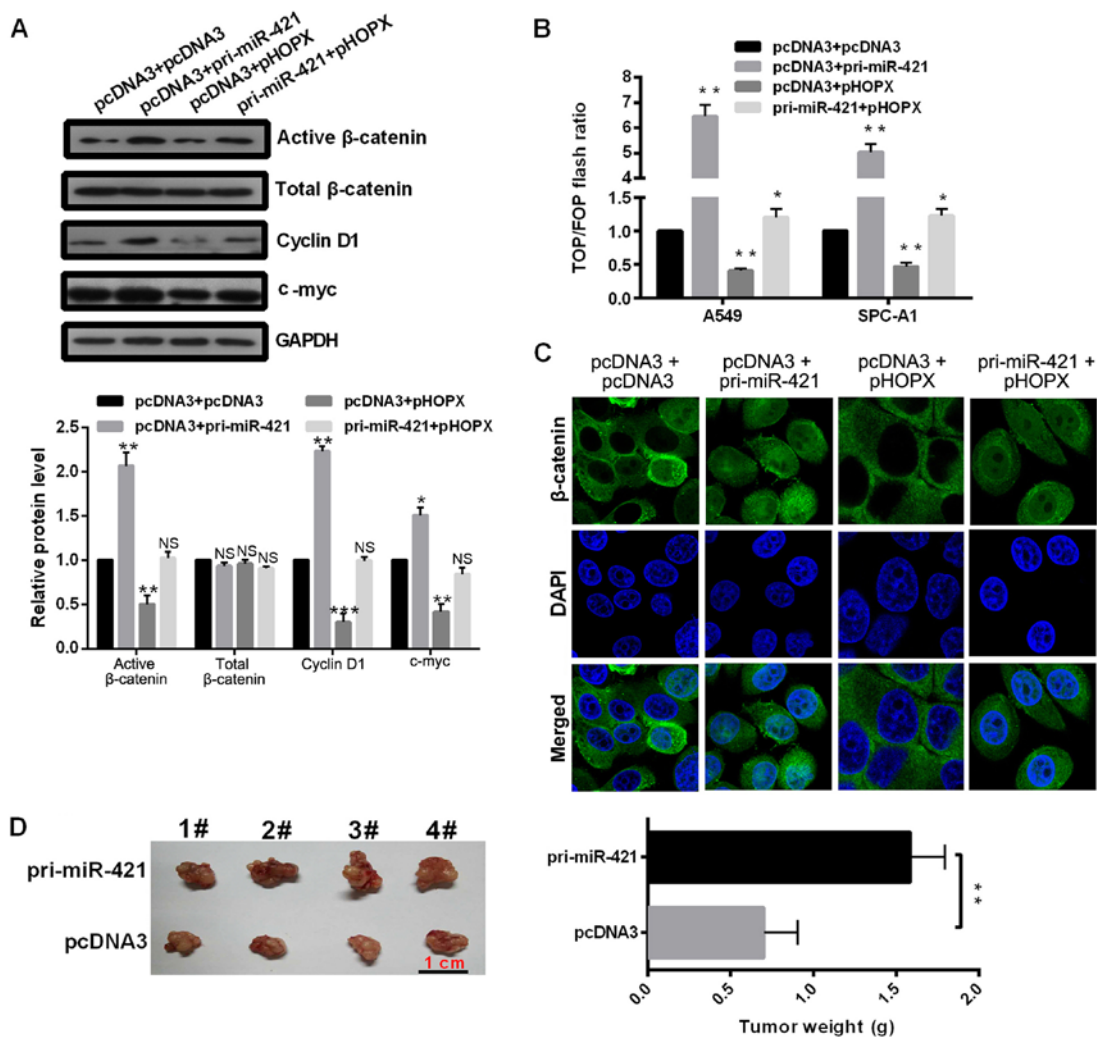
Figure 5. miR-421 regulates the Wnt/β-catenin signaling pathway by targeting HOPX. (A) Protein expression levels of active β-catenin, total β-catenin, cyclin D1 and c-myc were measured by western blot analysis. (B) TOP/FOP analysis. (C) β-catenin immunostaining (green) and DAPI staining (blue) were performed in A549 cells following transfection with the indicated plasmids. (D) Tumor size and weight were examined from mice xenografted with A549 cells that were transfected with pri-miR-421 or pcDNA3 negative control. Data are presented as the mean ± standard deviation; *P<0.05, **P<0.01, ***P<0.001. HOPX, homeodomain-only protein; pcDNA3, empty vector; pHOPX, HOPX overexpression vector; miR, microRNA; NS, not significant; pri, primary.

Subsequently, the effects of miR-421 and HOPX on the protein expression levels of cyclin D1 and c-myc were investigated, which are the downstream target genes of the Wnt signaling pathway. The results demonstrated that miR-421 overexpression significantly promoted and HOPX overexpression significantly inhibited the expression levels of cyclin D1 and c-myc compared with the pcDNA3 group (Fig. 5A). To further investigate whether the effects of miR-421 on Wnt/β-catenin signaling pathway are mediated by HOPX, pri-miR-421 and pHOPX plasmids were co-transfected into the cells. The results demonstrated that HOPX may attenuate the induction of the Wnt/β-catenin signaling pathway associated with miR-421. In addition, TOP/FOP reporter assay was performed and the results revealed that miR-421 overexpression increased the TOP/FOP flash ratio, but he ratio was suppressed by HOPX overexpression, compared with Control-transfected A549 and SPC-A1 cells (Fig. 5B). Immunofluorescence analysis indicated that miR-421 promoted and HOPX inhibited the nuclear distribution of β-catenin in A549 cells (Fig. 5C), indicating that miR-421

actives but HOPX inactivates the Wnt pathway. Finally, to confirm the role of miR-421 in vivo, a mouse xenograft model was generated using A549 cells transfected with either pcDNA3 or pri-miR-421 overexpression vector (Fig. 5D). miR-421 significantly increased tumor weight in nude mice, which suggested that miR-421 may promote the malignant phenotype of NSCLS in vivo.

Discussion

Previous studies have demonstrated that numerous molecules and processes are involved in the onset and development of NSCLC, including altered epigenetic regulation associated with miRNAs (20-22). miRNAs are involved in a variety of cellular processes in numerous human diseases, particularly in the development and progression of cancer. Several dysregulated miRNAs have been reported in NSCLC including miR-224, miR-107, miR-484 and miR-384 (8,23-27). In addition, evidence has indicated that miRNAs are aberrantly expressed in human cancers and may function as tumor suppressors

or oncogenes (28). miR-421 has been demonstrated to be dysregulated in certain cancers and functions with varying roles. For instance, Li *et al* (29) reported that upregulated expression of miR-421 is associated with poor prognosis in non-small-cell lung cancer. Zhang *et al* (30) also reported that MEG3/miR-421/E-cadherin regulatory axis may be a novel therapeutic target for breast cancer. Chen *et al* (31) reported that miR-421promoted nasopharyngeal carcinoma cell proliferation and anti-apoptosis and as a novel regulatory mechanism for inactivation of FOXO4 in nasopharyngeal carcinoma.

In the present study, the expression levels of miR-421 in NSCLC tissues and cell lines were analyzed and the results showed that miR-421 was upregulated. In addition, to investigate the biological roles of miR-421 in NSCLC, a series of functional experiments were performed. The present study demonstrated that overexpression of miR-421 promoted NSCLC cell growth, migration and invasion *in vitro*. Furthermore, the results of the present study demonstrated that miR-421 may promote the progression of the cell cycle. The expression levels of anti-apoptotic Bcl-2, and cleaved caspase-3 and cleaved PARP were investigated, and miR-421 was observed to increase the expression levels of Bcl-2, and inhibit the protein expression levels of cleaved caspase-3 and cleaved PARP. In addition, the role of miR-421 on the expression of E-cadherin and vimentin were analyzed in the present study; these proteins have been reported to serve an important role in tumor metastasis (32). The results of the present study indicated that miR-421 inhibited the protein expression of E-cadherin, but increased that of vimentin, thereby promoting cell migration and invasion via the EMT process. Furthermore, inhibition of miR-421 expression had opposing effects. In addition, miR-421 was also observed to promote tumor growth *in vivo* in the present study.

The target genes of miRNAs usually mediate their function. In the present study, the potential targets of miR-421 were predicted and HOPX was selected for further analysis. The HOPX gene is considered to be necessary for the regulation of cardiac growth and development (33). The downregulation of HOPX was reported to lead to cardiac hypertrophy and heart failure (33). HOPX usually functions as a transcriptional inhibitor (19,34,35). It has been reported that HOPX is downregulated in gastric cancer, esophageal squamous cell carcinoma and uterine endometrial cancer, due to silencing of the HOPX promoter through hyper methylation (36-38); however, further investigation into the function of HOPX in NSCLC is required.

Results from the present study revealed HOPX as a direct target of miR-421 in NSCLC. Contrary to miR-421, HOPX overexpression exhibited an inhibitory effect on the malignant phenotypes of NSCLC cells in the present study. Additionally, the rescue experiments revealed HOPX rescued the miR-421-mediated role on cell proliferation and metastasis-associated traits. Furthermore, the underlying molecular mechanism by which miR-421 affects the progression of NSCLC was investigated in the present study. miR-421 overexpression increased the protein expression levels of active β-catenin, cyclin D1 and c-myc, which indicated induction of the Wnt/β-catenin signaling pathway.

Taken together, the results of the present study indicated that miR-421 may function as an oncogene in the progression

of NSCLC through the downregulation of HOPX linking it to the Wnt/β-catenin signaling pathway. The findings of the present study may provide a novel insight into NSCLC progression and contribute to the development of novel diagnostic and treatment approaches for NSCLC.

Availability of data and materials

The analyzed data sets generated during the present study are available from the corresponding author on reasonable request.

Authors' contributions

HL conceived, designed, drafted and performed the experiments. CW, KG and JL performed the RT-qPCR, western blotting, EdU and Transwell assays and analyzed the data. RJ provided help in conceiving and designing the study and revising the manuscript. All authors approved the final manuscript.

Ethics approval and consent to participate

The present study was approved by the Ethical Review Committee of The First Hospital of Qinhuangdao S(ethics approval no. QHD20160235). Written informed consent was obtained from all enrolled patients.

Patient consent for publication

Not applicable.

Competing interests

The authors declare that they have no competing interests.

References

1. Siegel RL, Miller KD and Jemal A: Cancer statistics, 2017. CA Cancer J Clin 67: 7-30, 2017.
2. Chen W, Zheng R, Baade PD, Zhang S, Zeng H, Bray F, Jemal A, Yu XQ and He J: Cancer statistics in China, 2015. CA Cancer J Clin 66: 115-132, 2016.
3. Holdenrieder S and Stieber P: New challenges for laboratory diagnostics in non-small cell lung cancer. Cancer Biomark 6: 119-121, 2010.
4. Wood SL, Pernemalm M, Crosbie PA and Whetton AD: Molecular histology of lung cancer: From targets to treatments. Cancer Treat Rev 41: 361-375, 2015.
5. Marmarelis M, Thompson JC, Aggarwal C, Evans TL, Carpenter E, Cohen RB, Langer CJ and Bauml J: Emerging uses of circulating tumor DNA in advanced stage non-small cell lung cancer. Ann Transl Med 5: 380, 2017.
6. Laskin JJ and Sandler AB: State of the art in therapy for non-small cell lung cancer. Cancer Invest 23: 427-442, 2005.
7. Kim VN, Han J and Siomi MC: Biogenesis of small RNAs in animals. Nat Rev Mol Cell Biol 10: 126-139, 2009.
8. Hanahan D and Weinberg RA: Hallmarks of cancer: The next generation. Cell 144: 646-674, 2011.

9. Djuranovic S, Nahvi A and Green R: A parsimonious model for gene regulation by miRNAs. Science 331: 550-553, 2011.
10. Huntzinger E and Izaurralde E: Gene silencing by microRNAs: Contributions of translational repression and mRNA decay. Nat Rev Genet 12: 99-110, 2011.
11. Bartel DP: MicroRNAs: Target recognition and regulatory functions. Cell 136: 215-233, 2009.
12. Stahlhut C and Slack FJ: Combinatorial action of MicroRNAs let-7 and miR-34 effectively synergizes with erlotinib to suppress non-small cell lung cancer cell proliferation. Cell Cycle 14: 2171-2180, 2015.
13. Liu L, Cui S, Zhang R, Shi Y and Luo L: MiR-421 inhibits the malignant phenotype in glioma by directly targeting MEF2D. Am J Cancer Res 7: 857-868, 2017.
14. Ge X, Liu X, Lin F, Li P, Liu K, Geng R, Dai C, Lin Y, Tang W, Wu Z, et al: MicroRNA-421 regulated by HIF-1α promotes metastasis, inhibits apoptosis, and induces cisplatin resistance by targeting E-cadherin and caspase-3 in gastric cancer. Oncotarget 7: 24466-24482, 2016.
15. Livak KJ and Schmittgen TD: Analysis of relative gene expression data using real-time quantitative PCR and the $2^{-\Delta\Delta C_T}$ method. Methods 25: 402-408, 2001.
16. Long MJ, Wu FX, Li P, Liu M, Li X and Tang H: MicroRNA-10a targets CHL1 and promotes cell growth, migration and invasion in human cervical cancer cells. Cancer Lett 324: 186-196, 2012.
17. Weidenfeld K and Barkan D: EMT and stemness in tumor dormancy and outgrowth: Are they intertwined processes? Front Oncol 8: 381, 2018.
18. Polyak K and Weinberg RA: Transitions between epithelial and mesenchymal states: Acquisition of malignant and stem cell traits. Nat Rev Cancer 9: 265-273, 2009.
19. Jain R, Li D, Gupta M, Manderfield LJ, Ifkovits JL, Wang Q, Liu F, Liu Y, Poleshko A, Padmanabhan A, et al: HEART DEVELOPMENT. Integration of Bmp and Wnt signaling by Hopx specifies commitment of cardiomyoblasts. Science 348: aaa6071, 2015.
20. Wang Q, Jiang S, Song A, Hou S, Wu Q, Qi L and Gao X: HOXD-AS1 functions as an oncogenic ceRNA to promote NSCLC cell progression by sequestering miR-147a. Onco Targets Ther 10: 4753-4763, 2017.
21. Pan JY, Zhang F, Sun CC, Li SJ, Li G, Gong FY, Bo T, He J, Hua RX, Hu WD, et al: miR-134: A human cancer suppressor? Mol Ther Nucleic Acids 6: 140-149, 2017.
22. Liu X, Xu Y, Pang Z, Guo F, Qin Q, Yin T, Sang Y, Feng C, Li X, Jiang L, et al: Knockdown of SUMO-activating enzyme subunit 2 (SAE2) suppresses cancer malignancy and enhances chemotherapy sensitivity in small cell lung cancer. J Hematol Oncol 8: 67, 2015.
23. Zhang Z, Yang Y and Zhang X: MiR-770 inhibits tumorigenesis and EMT by targeting JMJD6 and regulating WNT/β-catenin pathway in non-small cell lung cancer. Life Sci 188: 163-171, 2017.
24. Wang L, Liu W, Zhang YP and Huang XR: The miR-224 promotes non-small cell lung cancer cell proliferation by directly targeting RASSF8. Eur Rev Med Pharmacol Sci 21: 3223-3231, 2017.
25. Lu C, Xie Z and Peng Q: MiRNA-107 enhances chemosensitivity to paclitaxel by targeting antiapoptotic factor Bcl-w in non small cell lung cancer. Am J Cancer Res 7: 1863-1873, 2017.
26. Li T, Ding ZL, Zheng YL and Wang W: MiR-484 promotes non-small-cell lung cancer (NSCLC) progression through inhibiting Apaf-1 associated with the suppression of apoptosis. Biomed Pharmacother 96: 153-164, 2017.
27. Fan N, Zhang J, Cheng C, Zhang X, Feng J and Kong R: MicroRNA-384 represses the growth and invasion of non-small-cell lung cancer by targeting astrocyte elevated gene-1/ Wnt signaling. Biomed Pharmacother 95: 1331-1337, 2017.
28. Zhang L, Huang J, Yang N, Greshock J, Megraw MS, Giannakakis A, Liang S, Naylor TL, Barchetti A, Ward MR, et al: microRNAs exhibit high frequency genomic alterations in human cancer. Proc Natl Acad Sci USA 103: 9136-9141, 2006.
29. Li Y, Cui X, Li Y, Zhang T and Li S: Upregulated expression of miR-421 is associated with poor prognosis in non-small-cell lung cancer. Cancer Manag Res 10: 2627-2633, 2018.
30. Zhang W, Shi S, Jiang J, Li X, Lu H and Ren F: LncRNA MEG3 inhibits cell epithelial-mesenchymal transition by sponging miR-421 targeting E-cadherin in breast cancer. Biomed Pharmacother 91: 312-319, 2017.
31. Chen L, Tang Y, Wang J, Yan Z and Xu R: miR-421 induces cell proliferation and apoptosis resistance in human nasopharyngeal carcinoma via downregulation of FOXO4. Biochem Biophys Res Commun 435: 745-750, 2013.
32. Rafael D, Doktorovová S, Florindo HF, Gener P, Abasolo I, Schwartz S Jr and Videira MA: EMT blockage strategies: Targeting Akt dependent mechanisms for breast cancer metastatic behaviour modulation. Curr Gene Ther 15: 300-312, 2015.
33. Trivedi CM, Cappola TP, Margulies KB and Epstein JA: Homeodomain only protein X is down-regulated in human heart failure. J Mol Cell Cardiol 50: 1056-1058, 2011.
34. Trivedi CM, Zhu W, Wang Q, Jia C, Kee HJ, Li L, Hannenhalli S and Epstein JA: Hopx and Hdac2 interact to modulate Gata4 acetylation and embryonic cardiac myocyte proliferation. Dev Cell 19: 450-459, 2010.
35. Palpant NJ, Wang Y, Hadland B, Zaunbrecher RJ, Redd M, Jones D, Pabon L, Jain R, Epstein J, Ruzzo WL, et al: Chromatin and transcriptional analysis of mesoderm progenitor cells identifies HOPX as a regulator of primitive hematopoiesis. Cell Rep 20: 1597-1608, 2017.
36. Yamashita K, Kim MS, Park HL, Tokumaru Y, Osada M, Inoue H, Mori M and Sidransky D: HOP/OB1/NECC1 promoter DNA is frequently hypermethylated and involved in tumorigenic ability in esophageal squamous cell carcinoma. Mol Cancer Res 6: 31-41, 2008.
37. Yamaguchi S, Asanoma K, Takao T, Kato K and Wake N: Homeobox gene HOPX is epigenetically silenced in human uterine endometrial cancer and suppresses estrogen-stimulated proliferation of cancer cells by inhibiting serum response factor. Int J Cancer 124: 2577-2588, 2009.
38. Ooki A, Yamashita K, Kikuchi S, Sakuramoto S, Katada N, Kokubo K, Kobayashi H, Kim MS, Sidransky D and Watanabe M: Potential utility of HOP homeobox gene promoter methylation as a marker of tumor aggressiveness in gastric cancer. Oncogene 29: 3263-3275, 2010.